Centrifuge modelling of dynamic response of soft clay

La modélisation en centrifuge de la réponse dynamique des argiles molles

T.KIMURA, Professor of Civil Engineering, Tokyo Institute of Technology, Tokyo, Japan
A.NAKASE, Professor of Civil Engineering, Tokyo Institute of Technology, Tokyo, Japan
J.TAKEMURA, Research Associate of Civil Engineering, Tokyo Institute of Technology, Tokyo, Japan
A.HIROOKA, Research Student of Civil Engineering, Tokyo Institute of Technology, Tokyo, Japan

SYNOPSIS Centrifuge model tests were conducted in 50g field using an electro-hydraulic earthquake simulator in order to study the dynamic stability of soft clay foundation under an embankment. Displacements fed to the base of a model container were sinusoidal and the amplitude was ±15mm in prototype scale. The effects of magnitude of seismicity, duration of an earthquake and the static factor of safety on deformations of foundation soil were investigated. The tests showed that clay foundation subjected to seismic loading experiences large deformations in wider areas than for static loading. It was found out that the deformations are larger for higher seismicity, longer loading duration and lower factor of safety. The sliding block analysis was carried out to predict the settlements of embankment by incorporating the results of cyclic triaxial tests into the analysis. The overall agreement between the prediction and measurement was satisfactory.

INTRODUCTION

Such structures as breakwaters or quay walls built on saturated soft clay often fail during an earthquake. A number of studies have been carried out to investigate the dynamic behaviour of soft clay and they have revealed various important characteristics of the soil under cyclic loading (Sangrey et al.,1969, Matsui et al.,1977). Most of these works are on an element of soil. Only few research works seem to have been conducted to study the dynamic behaviour of masses of clay soil. This is probably because of considerable difficulties in carrying out proper model tests under earthquake loading.

The centrifuge modelling technique has been attracting very wide attention in recent years because the similitude with respect to stress as well as geometry can be satisfied between a small scale model and a prototype. Kutter(1982) conducted centrifuge tests to study the stability of a clay embankment under model earthquakes.

The centrifuge research group at Tokyo Institute of Technology looked into the stability of soft clay under a sand embankment using a newly developed earthquake simulator. The group also carried out a series of cyclic triaxial tests on the clay used for the centrifuge model tests. The results were incorporated into the sliding block analysis in an attempt to predict the settlements of the embankment under earthquake loading.

CENTRIFUGE MODEL TESTS

Soil used for the centrifuge model tests is an artificial mixture with Ip of 10.2 made by mixing Kawasaki clay with crushed Toyoura sand. The physical properties of the soil are listed in Table I. Deaired slurry was poured into a centrifuge strong box and preliminary consolidation was conducted on the lab floor under the pressure of 9.8kPa. On completion of preliminary consolidation, surface markers were placed and eight to ten small pore pressure transducers were inserted into clay. The clay was once again consolidated on the lab floor under the pressure of 19.6kPa.

The earthquake simulator consists of a double acting hydraulic piston and a servo-valve (Kimura et al.,1988). A strong box which containing a model hangs from a pair of hanger rods attached to an outer box bolted to the loading platform of the centrifuge. The double acting hydraulic piston is fixed to the base plate of the outer box. The details of T.I.T. centrifuge and the earthquake simulator were described elsewhere (Kimura et al.,1984,1988).

Centrifuge consolidation was conducted for about three hours under 50g, achieving 95% consolidation. The estimated profile of undrained shear strength after consolidation is shown in Fig.1. A model embankment was built with zircon sand with Gs of 4.67 and angle of repose of 34° after stopping the centrifuge. The model was instrumented with an L.V.D.T. at the top of the embankment and three accelerometers at the top part of the box, at the surface of

TABLE I Physical Properties of Soil

Specific gravity	G_s	2.63
Plasticity index	I_p	10.2
Rate of strength increase	c_u/p	0.372
Angle of shearing resistance	ϕ'	37.3°

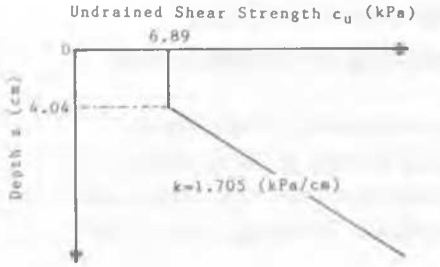

Fig.1 Estimated Profile of Undrained Shear Strength of Soil

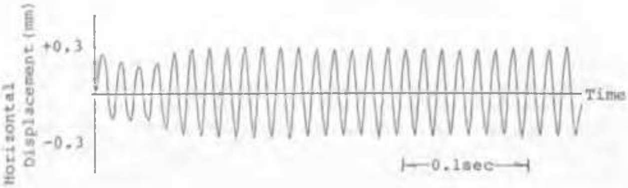

Fig.2 Input Displacements

foundation soil and in the embankment. The centrifuge was once again spun up to 50g and sinusoidal displacements as shown in Fig.2(+15mm in prototype scale) were given to the model. The test cases covered by this series of model tests are summarized in Table II. The only difference between DC1 and DC4 is the height of embankment or the static factor of safety. The three cases of DC2, DC4 and DC5 differ only in horizontal seismicity. The duration of model earthquake for DC3 is nearly twenty times as that of DC4.

CYCLIC TRIAXIAL TESTS

A series of cyclic triaxial tests was conducted on the same batch of clay as used for centrifuge tests. The tests consist of two stages; the first stage for cyclic loading and the second stage for shearing. The apparatus used for the tests is provided with an electro-hydraulic actuator which is controlled by a hydraulic servo-valve. A triaxial cell of double chamber type was employed so that the control of cell pressure for K_0 consolidation can be carried out easily. Axial deformations were measured with a displacement transducer of non-contact type. A triaxial specimen with 125mm in height and 50mm in diameter was trimmed from a block of clay consolidated under 133kPa.

The specimens consolidated in K_0 condition under the vertical pressure of 392kPa were subjected to stress-controlled cyclic loading. The tests were conducted for frequencies of 0.1 and 1Hz and for the number of loading cycles of 10 and 100 with stress amplitude level between 0.5 and 1.7. The stress amplitude level is defined as $\sigma_d/(q_f-q_0)$, where σ_d is the magnitude of applied dynamic stress, q_f is the deviator stress at static failure and q_0 is the deviator stress at the end of K_0 consolidation. The second stage of the tests was carried out after confirming that pore pressures generated by the first stage of the tests became stable.

TABLE II Test Cases

case	DC1	DC2	DC3	DC4	DC5
Frequency (Hz)	70(1.4)	100(2.0)	70(1.4)	70(1.4)	45(0.9)
Shaking time (sec)	0.4(20)	0.4(20)	7(350)	0.4(20)	0.4(20)
Amplitude (mm)	0.3(15)	0.3(15)	0.3(15)	0.3(15)	0.3(15)
Seisimicity	0.1	0.2	0.1	0.1	0.05
Height of embankment (cm)	2.6(130)	3.0(150)	3.0(150)	3.0(150)	3.0(150)
Fs (static)	1.33	1.19	1.19	1.19	1.19
Fd (dynamic)	0.89	0.65	0.85	0.85	1.00

( ) : prototype scale

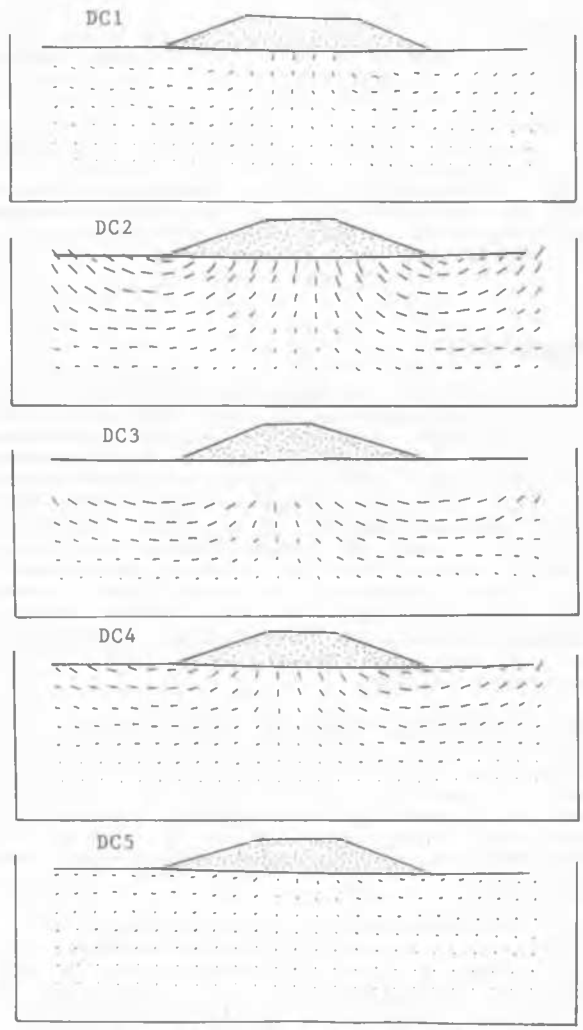

Fig.3 Observed Deformations

TEST RESULTS AND DISCUSSIONS

Deformations of foundation soil caused by model earthquakes are shown in Fig.3. In all the cases the deformations are generally very large and considerable deformations are seen even in areas far from the embankment. Normally in static loading a distinct failure plane appears and it stays at one fixed plane. In dynamic loading, however, load varies with time, giving rise to variation in stresses. As a result many failure planes appear, causing large deformations in wide areas. This implies that deformations of foundation soil are larger for higher horizontal seismicity and lower static factor of safety. This is confirmed by comparing the deformations in DC2, DC4 and DC5 with different seismicity and those in DC1 and DC4 with different static factor of safety.

It was thought that larger horizontal deformations might appear for higher seismicity, because inertia force exerted by input vibration is dominantly horizontal. The deformations for test case DC2 with higher seismicity, however, are more in vertical direction than those for DC4 with lower seismicity. This may be because greater vibration causes softening of soil beneath the embankment to a greater extent.

The dynamic stability of slopes or foundations is often evaluated with the pseudo-dynamic analysis which takes dynamic effects into account in the form of horizontal body force. The application of this conventional analysis gives rise to an identical factor of safety for DC3 and DC4 as shown in Table II. Test case DC3 with longer earthquake duration, however, shows larger deformations in wider areas. This demonstrates that the duration of an earthquake is also an important factor which controls the dynamic stability of foundation soil.

Typical variations of pore pressures observed during the tests are shown in Fig.4. In the areas beneath the embankment, pore pressures tend to decrease with the progress of vibration. As was already pointed out, soil beneath embankment softens by being subjected to vibration, resulting in large settlements of embankment. This in turn causes large lateral deformations as can be seen in DC2, DC3 and DC4. When this happens, confining pressures decrease inevitably, leading to decrease in pore pressures. Oscillation in pore pressures in the areas 1b, 2b and 3b may be because oscillatory change in stresses which are likely to occur in these areas.

Newmark(1965) proposed a useful method of predicting settlement of an embankment subjected to earthquake loading, known as the sliding block analysis. In this analysis a sliding part of an embankment is assumed as a rigid block on

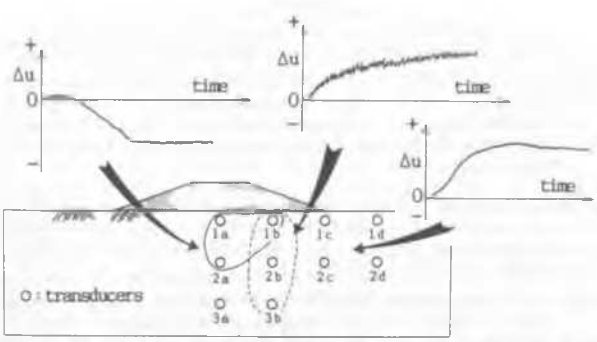

Fig.4 Variation of Pore-Water Pressures

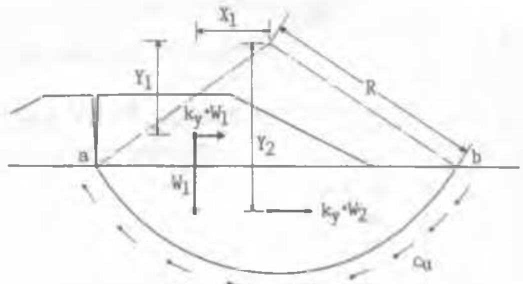

Fig.5(a) Mode of Failre Employed in Sliding Block Analysis

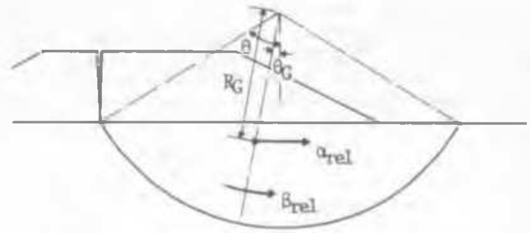

Fig.5(b) Accelerations of Sliding Block

a slope which starts sliding down along the slope when the horizontal acceleration of slope α_h exceeds a limiting acceleration α_y. The horizontal acceleration of the block itself α_{rel} is given by

$$\alpha_{rel} = \alpha_h - \alpha_y \qquad (1)$$

The minumum value of α_y was calculated for all the possible failure planes shown in Fig.5(a) and it was used in Eq.(1). This horizontal acceleration α_{rel} can be converted into the relative angular acceleration of the block β_{rel} by considering the equilibrium of moment and the angle of rotation of sliding block θ_{rel} is calculated from β_{rel} as

$$\theta_{rel} = \Sigma \int_{t_1}^{t_2} \{ \int_{t_1}^{t} \beta_{rel} dt \} dt \ , \ \beta_{rel} = \frac{\alpha_{rel} \cdot \cos\theta_G}{R_G} \qquad (2)$$

where θ_G is the angle between the line connecting the center of sliding arc with the gravitational center of sliding soil mass and the vertical and R_G is the distance between the two centers(Fig.5(b)). The summation sign is for considering all the waves of input oscillation, and the relative movement of the sliding block continues for the time interval between t_1 and t_2. Using θ_{rel} in Eq.(2), the settlement of the embankment is obtained as

$$S = R\{\cos(\theta - \theta_{rel}) - \cos\theta\} \qquad (3)$$

The settlement of the embankment was calculated by using Eq.(3) on the basis of the static undrained strength of clay obtained from static triaxial tests. The calculated settlements

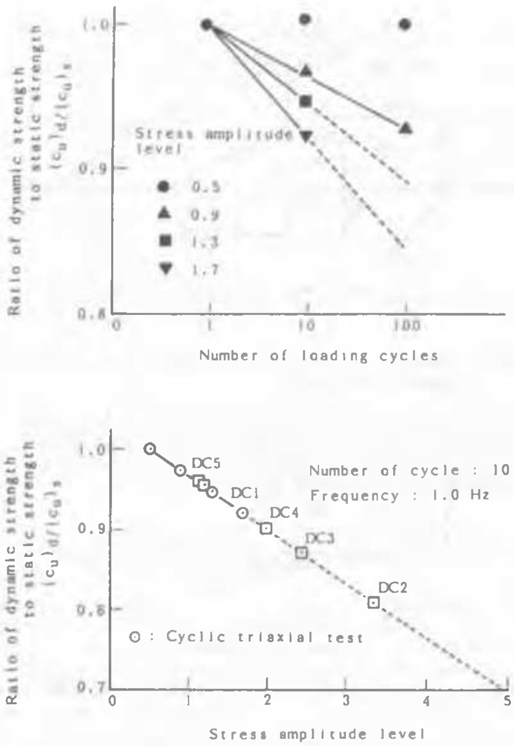

Fig.6 Results of Cyclic Triaxial Tests

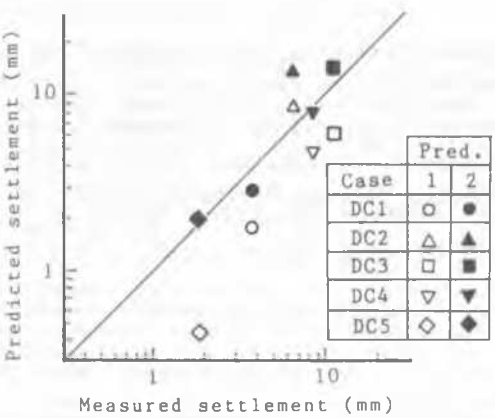

Fig.7 Comparision of Prediction of Settlements of Embankment with Measurement

(Prediction 1) are compared with measurement in Fig.7. The prediction is considerably smaller than measurement. This may be because decrease in undrained shear strength due to cyclic loading was not taken into account.

The results of cyclic triaxial tests carried out to see the reduction in undrained strength are summarized in Fig.6, which shows that the undrained strength decreases with the increase of the stress amplitude level and the number of loading cycles. This relationship was incorporated into the sliding block analysis (Prediction 2). The stress amplitude level was calculated from an average shear stress amplitude τ_d and an initial average shear stress τ_s by using $\tau_d/(c_u-\tau_s)$. The expressions for τ_d and τ_s are obtained by refering to Fig.5(a) as

$$\tau_d = \frac{k_h(W_1 \cdot Y_1 + W_2 \cdot Y_2)}{2R^2\theta} \qquad \tau_s = \frac{W_1 \cdot X_1}{2R^2\theta} \qquad (4)$$

where θ is one half of the angle of sliding mass and k_h is seismicity.

The calculated settlements are compared with the measured values in Fig.7, showing that the prediction taking into account the strength reduction compares well with measurements.

CONCLUSIONS

Following conclusions are drawn from this study.

(1) Clay foundation under an embankment experiences large deformations in wider areas in earthquake loading than in static loading.

(2) Deformations are larger for higher horizontal seismicity, longer duration of loading and lower static factor of safety.

(3) Clay beneath an embankment shows marked settlements for higher horizontal seisimicity, implying that this part of clay softens by vibration.

(4) The sliding block analysis into which reduction of undrained shear strength due to cyclic loading is incorporated gives reasonable prediction of settlements of embankments.

REFFERENCES

Kimura,T.,Kusakabe,O. and Saitoh,K. (1985). Geotechnical model tests of bearing capacity problems in a centrifuge. Geotechnique (35), 1, 33-45.

Kimura,T.,Takemura,J. and Saitoh,K. (1988). Development of an electro-hydraulic centrifuge earthquake simulator. Proc. the International Conf. on geotechnical centrifuge modelling,103-106,Paris,Balkema.

Kutter,B.L. (1982). Deformation of centrifuge models of clay embankments subjected earthquake. Proc. Conf. on Soil Dynamics and Earthquake Engineering,Vol.1,331-350, Southampton.

Matsui,T.,Ohara,H. and Ito,T. (1977). Effects of dynamic stress history on mechanical characteristics of saturated clays. Proc. JSCE, No257, 41-51.

Sangrey,D.A.,Henkel,D.J. and Esring,M.J. (1969). The effective stress response of a saturated clay soil to repeated loading. Canadian Geotech, Jour., 6, 3, 241-252.